Supplementary Information

Magneto-structural and theoretical insights into Ni_2Dy_2 butterfly single-molecule magnets with diverse anionic co-ligands

Anangamohan Panja,*[a,b] Zvonko Jagličić,[c] Daniel Aravena[d] Narayan Ch. Jana,[b] and Paula Brandão[e]

[a] *Department of Chemistry, Gokhale Memorial Girls' College, 1/1 Harish Mukherjee Road, Kolkata-700020, India. E-mail: ampanja@yahoo.co.in*

[b] *Department of Chemistry, Panskura Banamali College, Panskura RS, WB 721152, India*

[c] *Institute of Mathematics, Physics and Mechanics & Faculty of Civil and Geodetic Engineering, University of Ljubljana, Jadranska 19, 1000 Ljubljana, Slovenia*

[d] *Department of Materials Chemistry, Faculty of Chemistry and Biology, University of Santiago de Chile, Casilla 40, Correo 33, Santiago, Chile*

[e] *Department of Chemistry, CICECO-Aveiro Institute of Materials, University of Aveiro, 3810-193 Aveiro, Portugal*

Table S1: Crystal data and structure refinement parameters for complexes **1-5**.

	Complex **1**	Complex **2**	Complex **3**	Complex **4**	Complex **5**
Empirical formula	$C_{62}H_{57}Dy_2N_7Ni_2O_{19}$	$C_{76}H_{80}Dy_2N_6Ni_2O_{18}$	$C_{62}H_{60}Dy_2N_6Ni_2O_{16}S_2$	$C_{64}H_{76}Dy_2N_4Ni_2O_{25}$	$C_{70}H_{70}Dy_2N_4Ni_2O_{16}$
Formula weight	1646.56	1807.88	1651.7	1743.7	1665.72
Temperature/K	150	100.15	100.15	150	100.15
Crystal system	orthorhombic	triclinic	triclinic	monoclinic	triclinic
Space group	Pbca	P-1	P-1	C2/c	P-1
a/Å	14.3052(10)	11.1086(3)	11.0156(3)	24.470(5)	11.1635(3)
b/Å	16.0611(13)	12.5027(2)	11.4301(4)	12.5293(19)	12.2232(3)
c/Å	26.251(2)	14.5057(3)	14.6227(4)	22.778(5)	13.2329(4)
α/°	90	65.386(2)	67.037(3)	90	107.887(2)
β/°	90	88.710(2)	76.289(2)	106.826(9)	106.295(2)
γ/°	90	80.896(2)	64.293(3)	90	97.049(2)
Volume/Å^3	6031.4(8)	1806.41(7)	1522.34(9)	6684(2)	1605.66(8)
Z	4	1	1	4	1
ρ_{calc}g/cm^3	1.813	1.662	1.802	1.733	1.723
μ/mm^{-1}	3.146	2.633	3.179	2.849	13.503
F(000)	3272	910	822	3504	834
2Θ range for data collection/°	4.916 to 58.502	3.718 to 54.99	4.186 to 52.998	4.878 to 58.306	7.456 to 156.354
Reflections collected	315079	33561	26435	137934	26141
Independent reflections	8165 [R_{int} = 0.0435, R_{sigma} = 0.0109]	8083 [R_{int} = 0.0522, R_{sigma} = 0.0448]	6288 [R_{int} = 0.0499, R_{sigma} = 0.0404]	8989 [R_{int} = 0.0295, R_{sigma} = 0.0111]	6736 [R_{int} = 0.0682, R_{sigma} = 0.0547]
Data/restraints/parameters	8165/36/442	8083/0/478	6288/6/412	8989/3/482	6736/0/431
Goodness-of-fit on F^2	1.24	1.046	1.082	1.11	1.046
Final R indexes [I>=2σ (I)]	R_1 = 0.0468, wR_2 = 0.0980	R_1 = 0.0391, wR_2 = 0.1018	R_1 = 0.0350, wR_2 = 0.0803	R_1 = 0.0161, wR_2 = 0.0405	R_1 = 0.0478, wR_2 = 0.1223
Final R indexes [all data]	R_1 = 0.0641, wR_2 = 0.1124	R_1 = 0.0447, wR_2 = 0.1047	R_1 = 0.0521, wR_2 = 0.0882	R_1 = 0.0174, wR_2 = 0.0415	R_1 = 0.0538, wR_2 = 0.1266
Largest diff. peak/hole / e Å^{-3}	2.70/-1.79	2.39/-1.19	2.60/-0.98	0.71/-0.65	1.57/-1.29

Table S2. Selected bond distances around the metal centers and the birding angles in **1-5**.

	1	**2**	**3**	**4**	**5**
Dy–O(phenoxide)	2.149(4)	2.191(3)	2.195(3)	2.2044(11)	2.167(3)
	2.313(4)	2.285(3)	2.280(3)	2.2568(11)	2.247(3)
	2.332(4)	2.366(3)	2.313(3)	2.3859(11)	2.296(3)
	2.404(4)	2.442(3)	2.410(3)	2.4091(11)	2.355(3)
Dy–O(methoxy)	2.495(5)	2.522(3)	2.529(3)	2.5552(12)	2.538(3)
Dy–N(imine)	2.402(5)	2.446(4)	2.467(3)	2.4624(13)	2.443(4)
Dy–O(nitrate or	2.456(5)	2.356(3)	-	2.3936(12)	2.286(3)
carboxylate)	2.497(5)	2.389(4)			
Dy–O(water)	-	-	2.408(3)	2.3991(14)	-
			2.448(3)		
Ni–O(phenoxide)	2.007(4)	2.010(3)	2.022(3)	2.0086(11)	1.988(3)
	2.061(3)	2.050(3)	2.066(3)	2.0818(11)	2.073(3)
	2.103(4)	2.097(3)	2.107(3)	2.1006(11)	2.114(3)
	2.127(4)	2.099(3)	2.147(3)	2.1271(11)	2.117(3)
Ni–N(imine)	1.997(5)	2.006(4)	2.022(3)	2.0109(13)	2.008(4)
Ni−N/O(other)	2.115(4)	2.106(3)	2.075(4)	2.0789(12)	2.031(4)
Ni···Ni	3.188(1)	3.1491(8)	3.2553(7)	3.2012(6)	3.189(1)
Ni···Dy	3.444(3)	3.4943(6)	3.4665(5)	3.3942(6)	3.319(1)
	3.492(3)	3.4989(8)	3.4906(5)	3.5328(9)	3.4352(8)
<Dy–O–Ni	98.7(1)-	100.3(1)-	98.9(1)-	97.40(4)-	95.7(1)-
	107.6(2)º	108.9(1)º	108.3(1)º	105.31(5)º	103.5(2)º
<Ni–O–Ni	97.8(1)º	97.3(1)º	99.8(1)º	98.44(4)º	97.8(2)º

Table S3. Shape analysis for Dy^{III} centers in **1-4.**

Label	Shape	Symmetry	**1**	**2**	**3**	**4**
			Dy1	Dy1	Dy1	Dy1
OP-8	Octagon	D_{8h}	33.445	33.385	31.844	31.938
HPY-8	Heptagonal pyramid	C_{7v}	21.579	22.242	22.834	23.056
HBPY-8	Hexagonal bipyramid	D_{6h}	15.521	12.513	13.787	14.473
CU-8	Cube	Oh	11.826	8.158	9.693	9.709
SAPR-8	**Square antiprism**	**D_{4d}**	**3.260**	**2.956**	**2.010**	**2.625**
TDD-8	**Triangular dodecahedron**	**D_{2d}**	**2.527**	**1.223**	**2.373**	**1.182**
JGBF-8	Johnson gyrobifastigium J26	D_{2d}	13.417	12.977	12.248	13.506
JETBPY-8	Johnson elongated triangular bipyramid J14	D_{3h}	26.784	26.793	26.403	27.066
JBTPR-8	**Biaugmented trigonal prism J50**	**C_{2v}**	**2.935**	**2.441**	**1.854**	**2.065**
BTPR-8	**Biaugmented trigonal prism**	**C_{2v}**	**2.571**	**2.116**	**1.495**	**1.683**
JSD-8	Snub diphenoid J84	D_{2d}	3.870	4.303	3.492	3.786
TT-8	Triakis tetrahedron	Td	12.352	8.915	10.303	10.409
ETBPY-8	Elongated trigonal bipyramid	D_{3h}	22.789	24.756	24.513	24.372

Table S4. Shape analysis for Dy^{III} centers in **5.**

Label	Shape	Symmetry	**5**
HP-7	Heptagon	D_{7h}	31.453
HPY-7	Hexagonal pyramid	C_{6v}	21.163
PBPY-7	**Pentagonal bipyramid**	**D_{5h}**	**2.031**
COC-7	Capped octahedron	C_{3v}	7.527
CTPR-7	Capped trigonal prism	C_{2v}	5.870
JPBPY-7	Johnson pentagonal bipyramid J13	D_{5h}	4.747
JETPY-7	Johnson elongated triangular pyramid J7	C_{3v}	17.445

Table S5. Extracted parameters from the least-square fitting of the Cole-Cole plots of **1** considering generalized Debye model at zero dc field.

T (K)	χ_S	$\Delta\chi$	τ(s)	α

	(emu/mol)	(emu/mol)		
2	0.50692	29.95964	0.04645	0.16491
2.15	0.56604	27.55135	0.02692	0.16105
2.4	0.66208	24.33121	0.01258	0.15801
2.6	0.73923	22.01671	0.00692	0.15666
2.8	0.80538	20.01597	0.00403	0.15651
3	0.866	18.27788	0.00246	0.157
3.2	0.92088	16.79119	0.00158	0.15728
3.4	0.97887	15.48715	0.00106	0.15685
3.6	1.02157	14.29931	7.28E-04	0.15485
3.8	1.07454	13.21141	5.31E-04	0.15432
4	1.12442	12.18736	4.00E-04	0.14986
4.2	1.14692	11.32284	3.11E-04	0.15015
4.4	1.14159	10.54566	2.47E-04	0.1486
4.6	1.15755	9.8147	2.03E-04	0.14562
4.8	1.14134	9.19789	1.69E-04	0.14395
5	1.11365	8.65548	1.44E-04	0.1437

Table S6. Extracted parameters from the least-square fitting of the Cole-Cole plots of **2** considering generalized Debye model at zero dc field.

T (K)	χ_S (emu/mol)	$\Delta\chi$ (emu/mol)	τ(s)	α
2	3.39709	22.50994	0.00338	0.33986
2.15	3.3279	20.73675	0.00198	0.32631
2.4	3.24024	18.35117	9.65E-04	0.31105
2.6	3.19086	16.60225	5.64E-04	0.30008
2.8	3.17628	15.05952	3.52E-04	0.29092
3	3.16693	13.7005	2.32E-04	0.28351
3.2	3.15808	12.53356	1.61E-04	0.27769
3.4	3.21873	11.42852	1.18E-04	0.27085
3.6	3.26888	10.40143	8.84E-05	0.2632
3.8	3.27986	9.51244	6.86E-05	0.2589

Table S7. Extracted parameters from the least-square fitting of the Cole-Cole plots of **3** considering generalized Debye model at zero dc field.

T (K)	χ_S (emu/mol)	$\Delta\chi$ (emu/mol)	τ(s)	α

2	0.61192	10.65641	0.00139	0.36702
2.15	0.26087	10.3573	7.51E-04	0.37082
2.4	0	9.75511	3.52E-04	0.36597
2.6	0	9.12132	2.09E-04	0.35881
2.8	0	8.57545	1.34E-04	0.35648
3	0	8.08516	8.96E-05	0.35784
3.2	0	7.65319	6.41E-05	0.35991
3.4	0	7.25691	4.78E-05	0.35639
3.6	0	6.87382	3.70E-05	0.34813
3.8	0	6.52732	2.92E-05	0.3421
4	0	6.20395	2.43E-05	0.33145
4.2	0	5.91443	2.06E-05	0.32459

Table S8. Extracted parameters from the least-square fitting of the Cole-Cole plots of **4** considering generalized Debye model at zero dc field.

T (K)	χ_S (emu/mol)	$\Delta\chi$ (emu/mol)	τ(s)	α
2	0.34514	26.20395	0.319	0.27043
2.15	0.41908	23.30051	0.14467	0.24975
2.4	0.49885	20.03839	5.15E-02	0.23024
2.6	0.54885	17.83058	2.34E-02	0.21928
2.8	0.61608	16.12335	1.16E-02	0.2106
3	0.6556	14.59775	6.20E-03	0.20542
3.2	0.70975	13.28463	3.56E-03	0.19893
3.4	0.74097	12.1553	2.13E-03	0.19479
3.6	0.78953	11.10632	1.33E-03	0.18866
3.8	0.85039	10.15947	8.85E-04	0.1819
4	0.87841	9.33228	6.10E-04	0.17607
4.2	0.91849	8.59125	4.40E-04	0.1711
4.4	0.95629	7.91957	3.30E-04	0.16345
4.6	0.96869	7.3423	2.55E-04	0.15757
4.8	0.99683	6.80249	2.03E-04	0.15062
5	1.00686	6.33014	1.65E-04	0.14614
5.5	1.02873	5.31776	1.08E-04	0.13066
6	0.95475	4.60744	7.64E-05	0.12261
6.5	0.97911	3.96895	6.08E-05	0.11138
7	0.76025	3.67968	4.65E-05	0.11189
7.5	0.60208	3.41386	3.78E-05	0.10972

Table S9. Extracted parameters from the least-square fitting of the Cole-Cole plots of **5** considering generalized Debye model at zero dc field.

T (K)	χ_S (emu/mol)	$\Delta\chi$ (emu/mol)	τ(s)	α

2	0.65741	25.22575	0.0164	0.15865
2.15	0.68431	23.08913	0.00782	0.15216
2.4	0.71332	20.31123	0.00295	0.1443
2.6	0.73265	18.34621	0.00144	0.13945
2.8	0.75857	16.66487	7.66E-04	0.13521
3	0.78565	15.20011	4.43E-04	0.13173
3.2	0.81841	13.94257	2.76E-04	0.12845
3.4	0.87878	12.83429	1.82E-04	0.12337
3.6	1.01409	11.73698	1.27E-04	0.11424
3.8	1.14041	10.72886	9.28E-05	0.10595
4	1.25862	9.8084	7.05E-05	0.0993
4.2	1.7263	8.63608	5.80E-05	0.09311
4.4	2.00996	7.7136	4.91E-05	0.08408
4.6	2.09485	7.05946	4.15E-05	0.07862
4.8	2.17326	6.46776	3.59E-05	0.07321
5	2.06842	6.10428	3.03E-05	0.07335

Table S10. Magnetic data and structural features of $Ni^{II}_2Dy^{III}_2$ butterfly complexes.

Complex[a]	Butterfly type	Dy center geometry	magnetic interaction	χ''_M signal	U_{eff}/K	Applied field/Oe	Ref.
$(Et_3NH_2)_2[Ni_2Dy_2(OH)_2(Piv)_{10}]$	Type-I	square antiprism (D_{4d})	AF	yes	20.0	0	S1
$[Ni_2Dy_2(L^3)_4(NO_3)_2(DMF)_2]$	Type-I	square antiprism (D_{4d})	F	yes	18.5	0	S2
$[Ni_2Dy2(L^3)_4(NO_3)_2(MeOH)_2]$	Type-I	square antiprism (D_{4d})	F	yes	21.3	0	S2

					28.5	4000	
$[Ni_2Dy_2(L^4)_4(NO_3)_2(H_2O)_2]$	Type-I	triangular dodecahedron (D_{2d})	F	yes	36.0	0	S3
$[Ni_2Dy_2(H_2L^5)_2(MeO)_2(MeCN)_2(NO_3)_4]$	Type-I	capped square antiprism (C_{4v})	F	yes	48.5	0	S4
$[Ni_2Dy_2(H_2L^6)_2(MeO)_2(MeCN)_2(NO_3)_4]$	Type-I	capped square antiprism (C_{4v})	F	yes	57.0	0	S4
$[Dy_2Ni_2(L^7)_2(\mu_3\text{-}OCH_3)2(\mu_{1,3}\text{-}PhCO_2)_2(PhCO_2)_2(MeOH)_4]\cdot 2CH_3OH$	Type-I	trigonal dodecahedron(D_{2d})	F	yes	-	-	S5
$[Ni_2Dy_2(L^8)_4(Ac)_2(DMF)_2]\cdot 3CH_3CN$	Type-I	square antiprism (D_{4d})	F	yes	18	0	S6
$Dy_2Ni_2(NO_3)_4L^9(\mu_3\text{-}OCH_3)_2\cdot 2(CH_3CN)$	Type-I	capped square antiprism (C_{4v})	F	Yes, no maximum	-	-	S7
$[\{L'_2{}^{10}\{Ni(MeOH)(\mu\text{-}OAc)\}_2(\mu_3\text{-}MeO)_2Ni_2\}$	Type-II	square antiprism (D_{4d})	F	no	-	-	S8
$Ni_2Dy_2(HL^{11})_2(\mu_3\text{-}OH)_2(piv)_6]\cdot 2CH_3CN$	Type-II	trigonal dodecahedron (D_{2d})	weak	no	-	-	S9
$[Ni_2Dy_2(HL^{12})_2(\mu_3\text{-}OH)_2(piv)_6]\cdot 2CH_3CN$	Type-II	trigonal dodecahedron (D_{2d})	weak	no	-	-	S9
1	Type-I	trigonal dodecahedron (D_{2d})	F	yes	19.9	0	This work
2	Type-I	trigonal dodecahedron (D_{2d})	F	yes	16.5	0	This work
3	Type-I	Biaugmented trigonal prism	F	yes	16.1	0	This work
4	Type-I	trigonal dodecahedron (D_{2d})	F	yes	25.5	0	This work
5	Type-I	Pentagonal bipyramid (D_{5h})	F	yes	21.4	0	This work

[a] Ligand abbreviations: H_2L^1 = (*E*)-2-(2-hydroxy-3-methoxybenzylideneamino)phenol; H_2L^2 = (E)-2-ethoxy-6-(((2-hydroxyphenyl)imino)methyl)phenol; H_4L^3 = 2-(((2- hydroxy-3-methoxyphenyl)methylene)amino)-2-(hydroxymethyl)- 1,3-propanediol; H_4L^4 = 2-(2,3-dihydroxpropyliminomethyl)-6-methoxyphenol; H_4L^5 = 2-[{(2-hydroxybenzyl)imino}methyl]-6-methoxyphenol; H_4L^6 = (E)-2-((2-hydroxy-3-methoxybenzylidene)amino)-4-methylphenol; H_4L^7 = methyl 3-methoxysalicylate; H_4L^8 = 3-{(2-hydroxy-3-methoxybenzylidene)amino}-2-(2-hydroxy-3-methoxyphenyl)-2,3-dihydroquinazolin-4(1*H*)-one; H_4L^9 = (*E*)-2-ethoxy-6-(((2-hydroxyphenyl)imino)methyl)phenol); H_4L^{10} = trans-1,2-di-aminocyclohexane-N,N,N',N'-tetraacetic acid; H_2L^{11} = 2-[(2-hydroxymethyl-phenylimino)methyl]-6-methoxyphenol; H_2L^{12} = 2-[(2-hydroxymethyl-phenylimino)methyl]-6-ethoxyphenol.

References

S1. S1. E. Moreno Pineda, N. F. Chilton, F. Tuna, R. E. P. Winpenny and E. J. L. McInnes, *Inorg. Chem.*, **2015**, *54*, 5930–5941.

S2. K. C. Mondal, G. E. Kostakis, Y. Lan, W. Wernsdorfer, C. E. Anson and A. K. Powell, *Inorg. Chem.*, **2011**, *50*, 11604–11611.

S3. S. Mandal, S. Ghosh, D. Takahashi, G. Christou and S. Mohanta, *Eur. J. Inorg. Chem.*, **2018**, *2018*, 2793–2804.

S4. H. H. Zou, L. B. Sheng, F. P. Liang, Z. L. Chen and Y. Q. Zhang, *Dalton Trans.*, **2015**, *44*, 18544–18552.

S5. A. Bhanja, R. Herchel, E. Moreno-Pineda, A. Khara, W. Wernsdorfer and D. Ray, *Dalton Trans.*, **2021**, *50*, 12517–12527.

S6. G.-P. Li, H.-Z. Tang, R.-C. Gao, Y.-Y. Wang, X. Sun and K. Zhang, *Cryst. Growth Des.*, **2023**, *23*, 1575–1580.

S7. N. Qiao, X. Y. Xin, X. F. Guan, C. X. Zhang and W. M. Wang, *Inorg. Chem.*, **2022**, *61*, 15098–15107.

S8. A. Chakraborty, N. Ahmed, J. Ali, S. Moorthy, J. Goura, S. K. Singh, G. Rogez and V. Chandrasekhar, *Dalton Trans.*, **2022**, *51*, 14721–14733.

S9. N. C. Jana, A. Escuer, R. Herchel, J. Serra, R. Nandy and A. Panja, *Cryst. Growth Des.*, **2024**, *24*, 6492–6502.

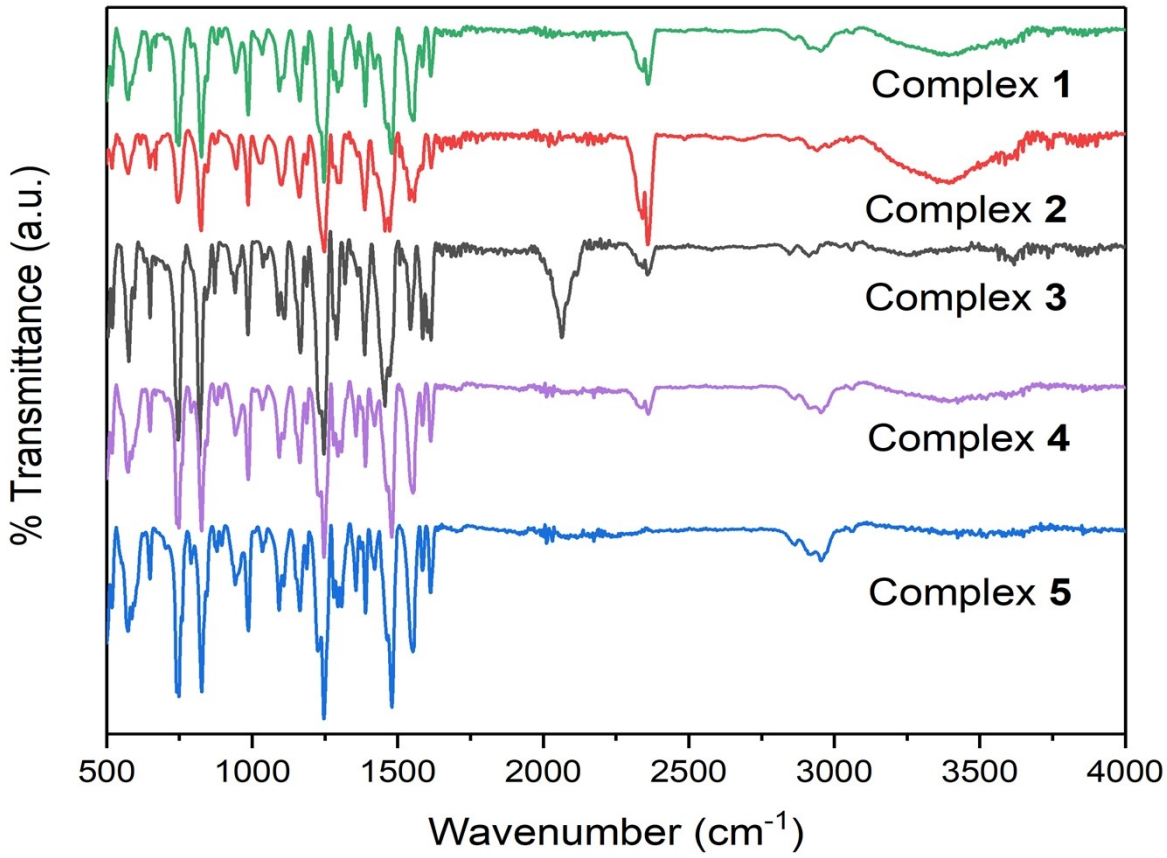

Fig. S1. IR spectra of complexes **1–5**.

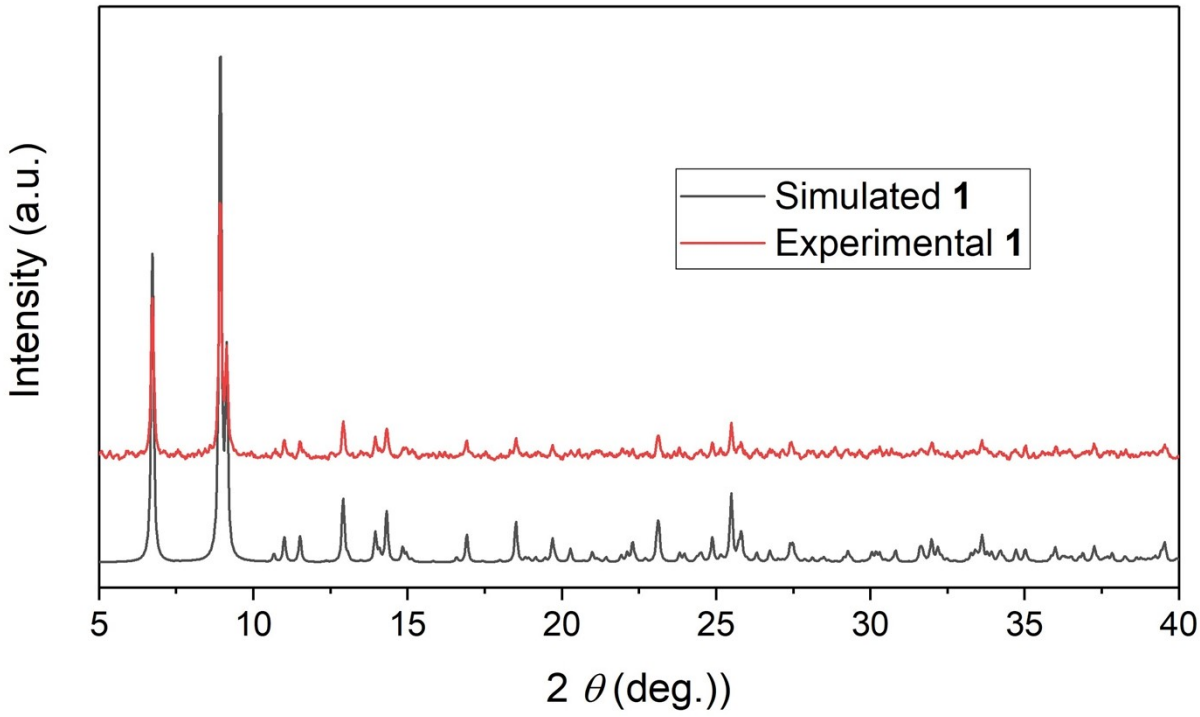

Fig. S2. PXRD data for complex **1**.

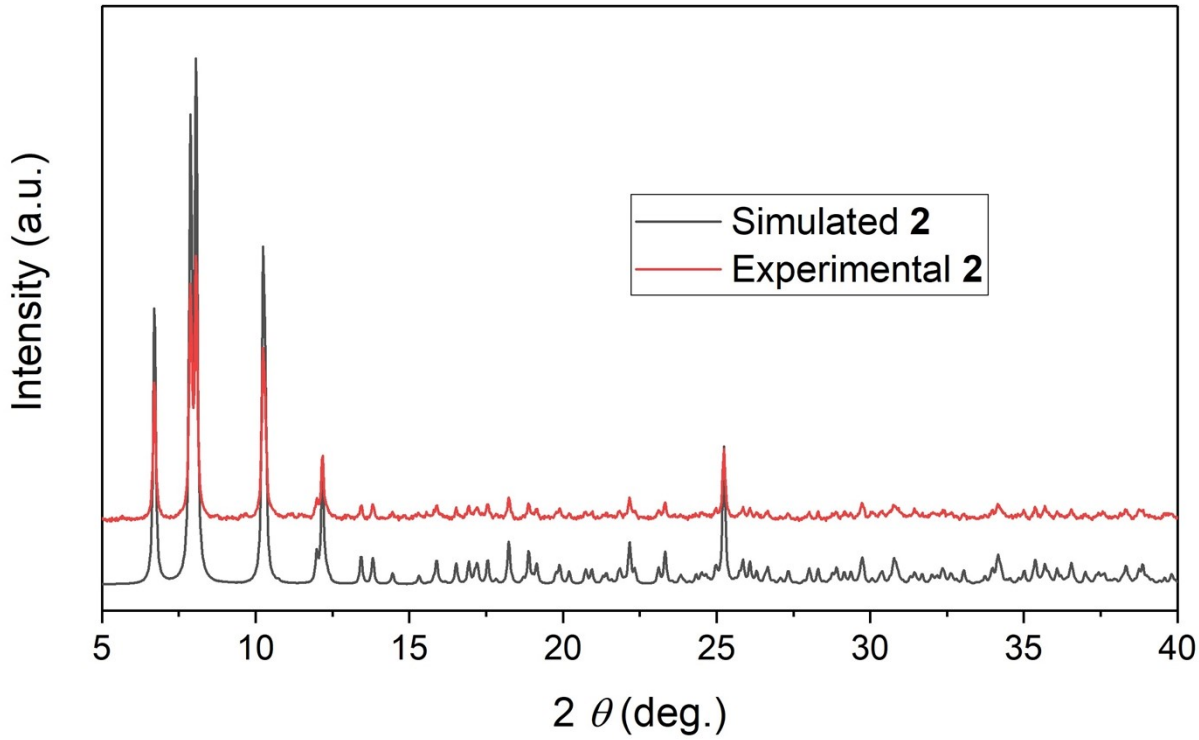

Fig. S3. PXRD data for complex **2**.

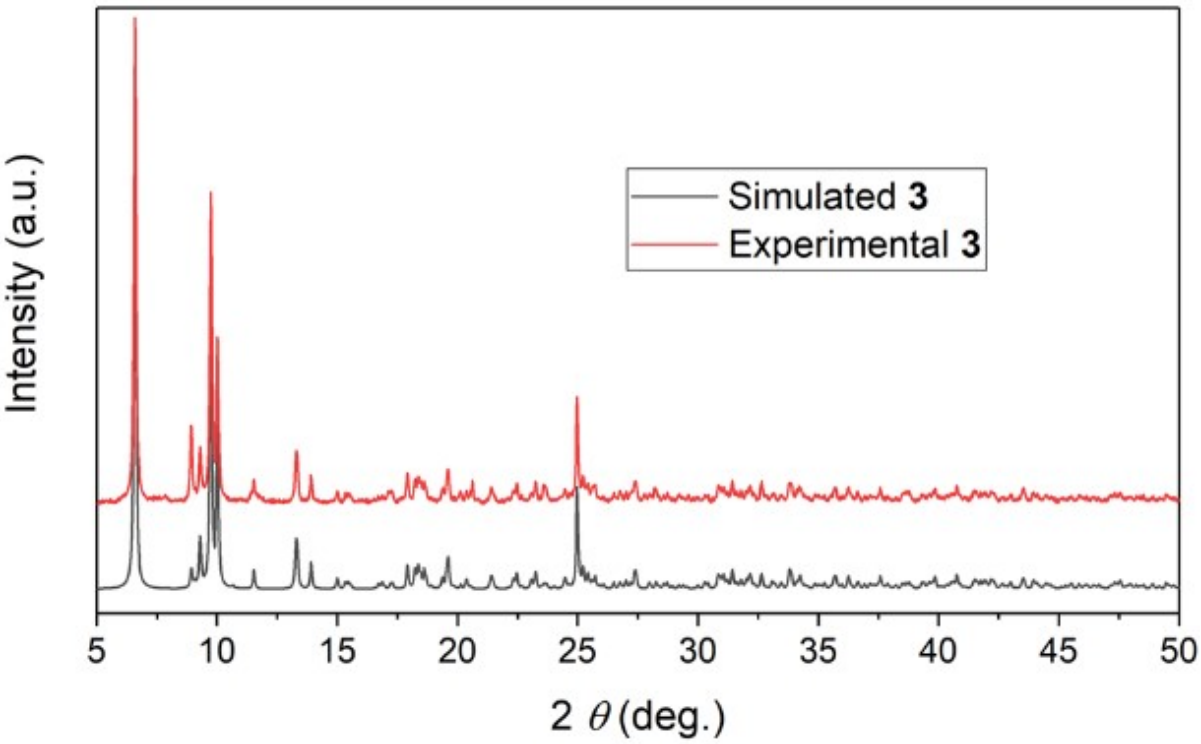

Fig. S4. PXRD data for complex **3**.

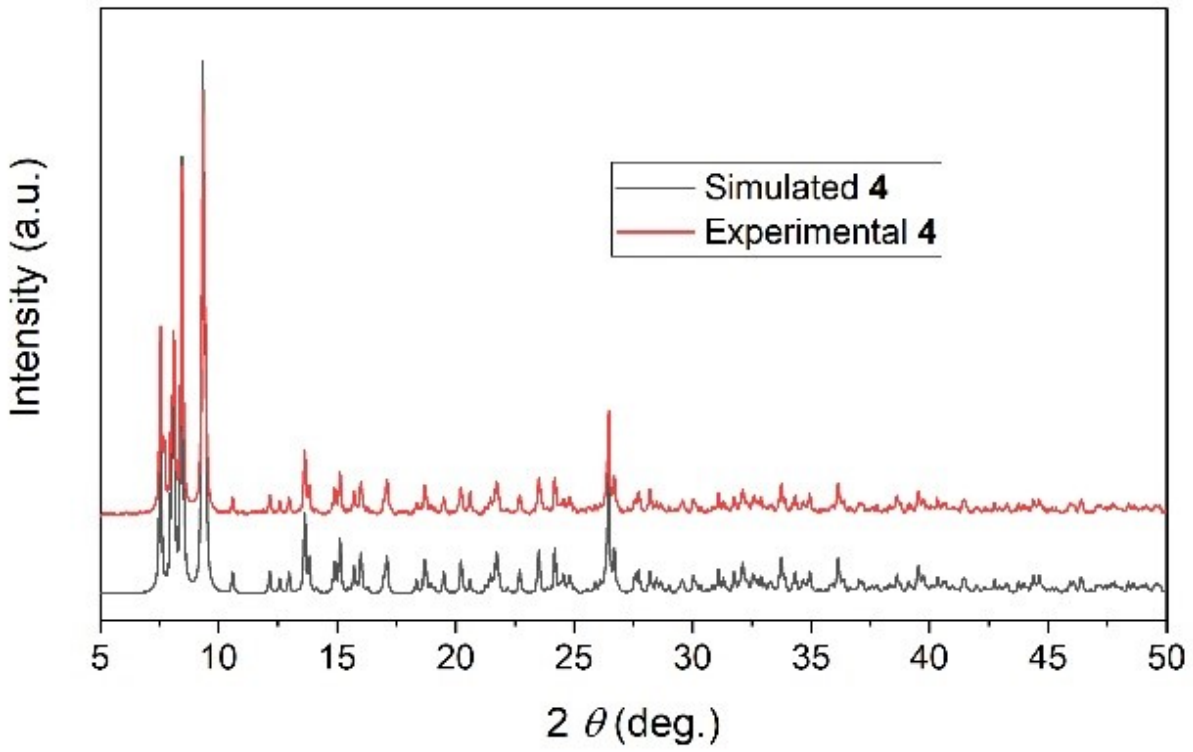

Fig. S5. PXRD data for complex **4**.

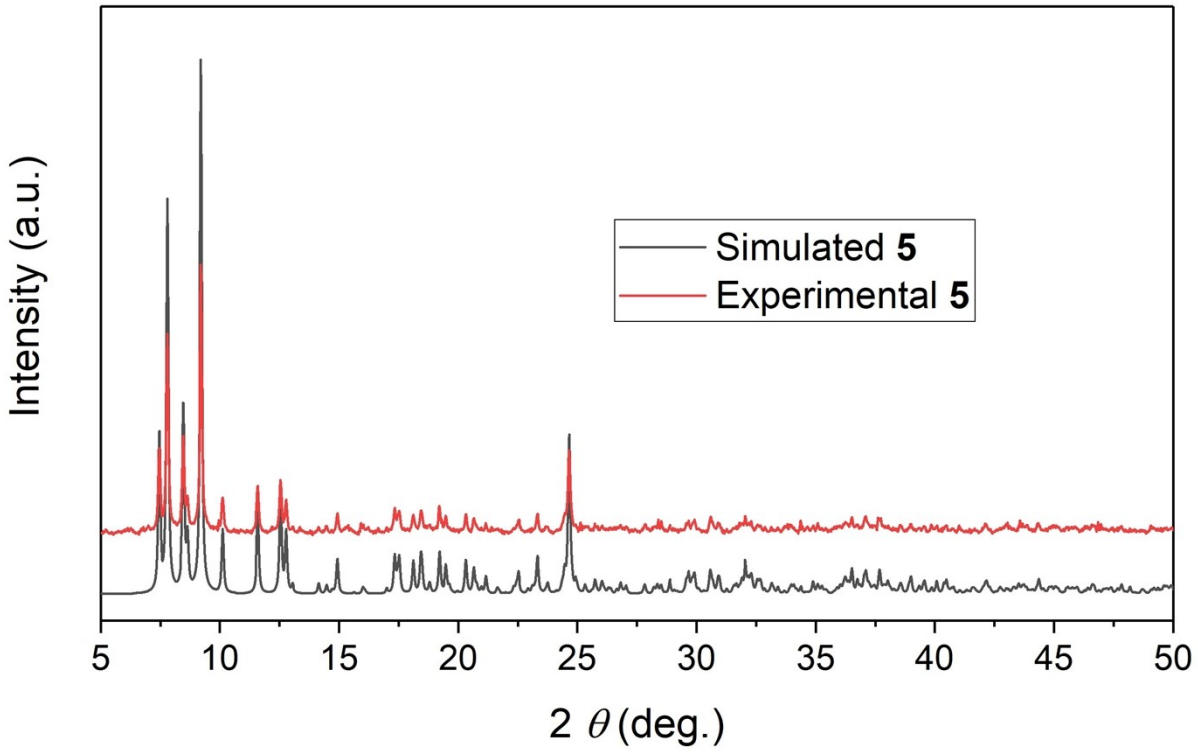

Fig. S6. PXRD data for complex **5**.

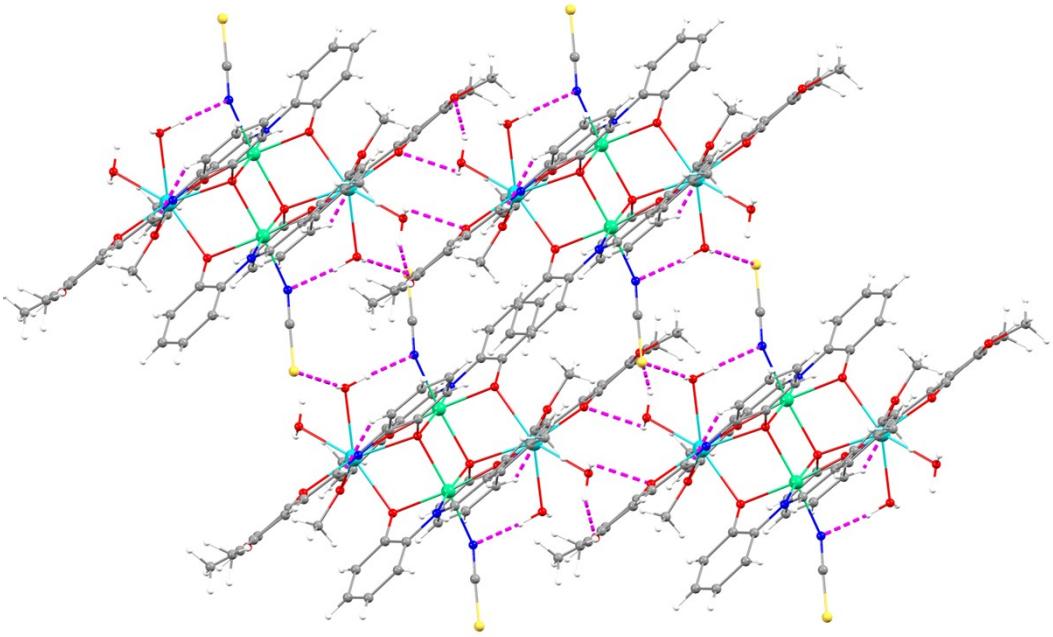

Fig. S7. Crystal packing of **3** showing extensive hydrogen bonding interaction.

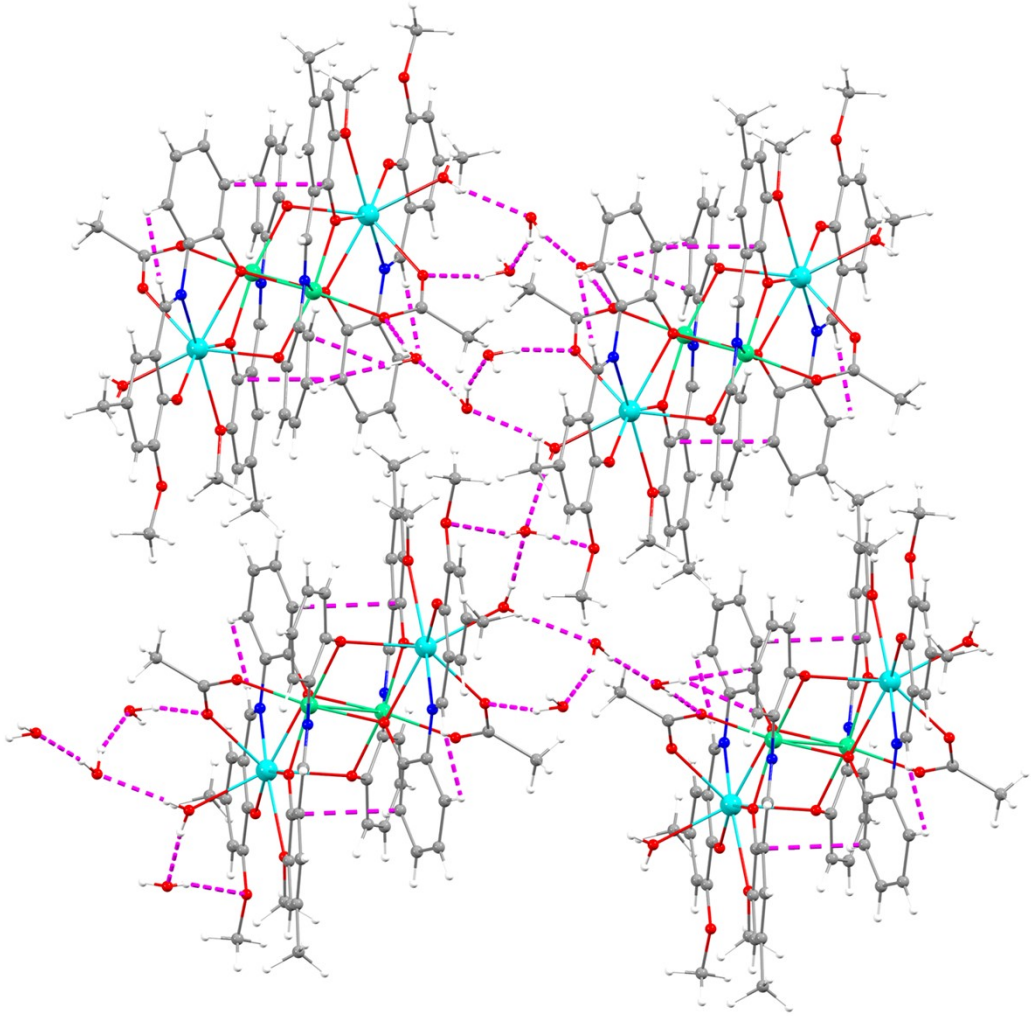

Fig. S8. Crystal packing of **2** showing a complex-network of hydrogen bonding interaction.

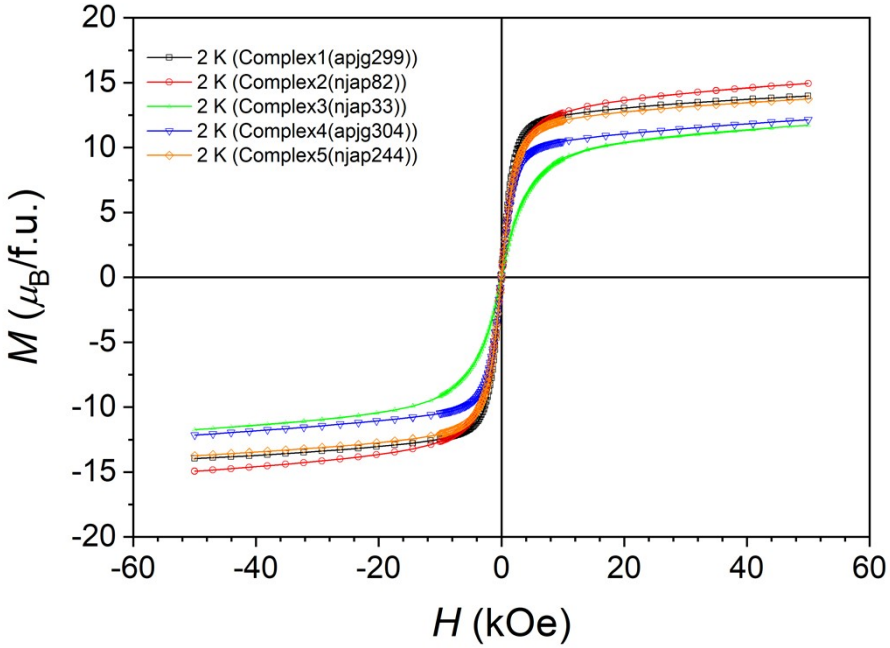

Fig. S9. Isothermal field-dependent magnetization plots for complexes **1–5**, recorded at 2 K in the magnetic field range ± 50 kOe.

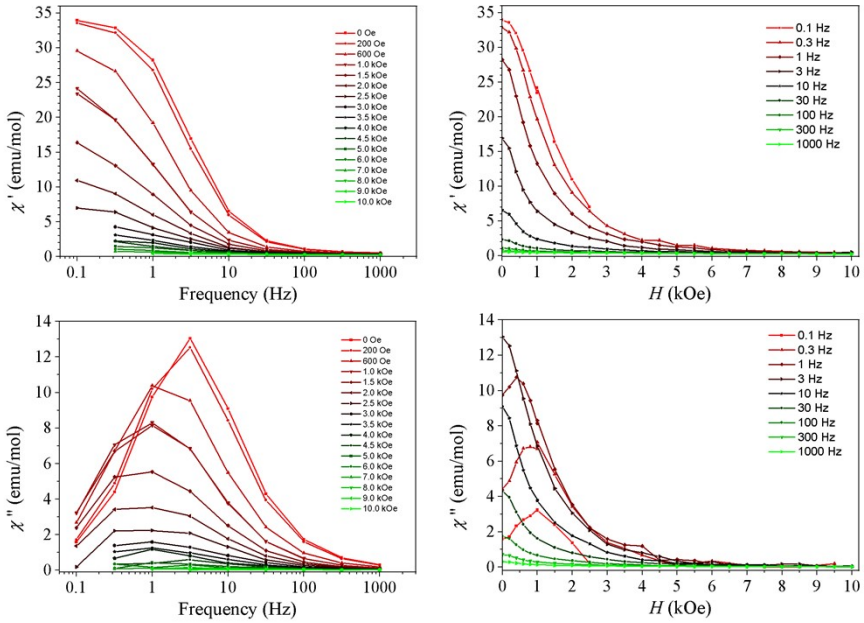

Fig. S10. Field dependence AC magnetic data for complex **1** at temperature T = 2 K.

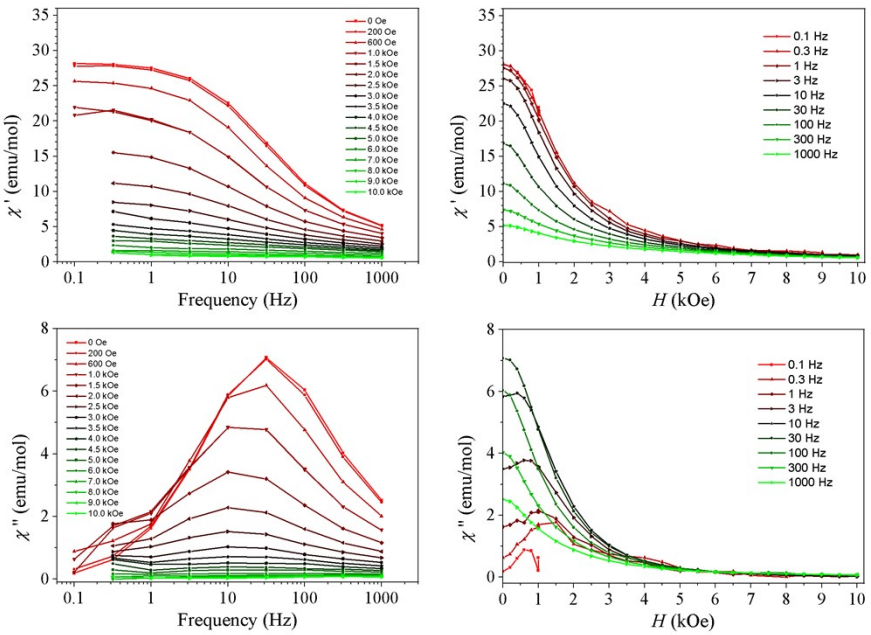

Fig. S11. Field dependence AC magnetic data for complex **2** at temperature T = 2 K.

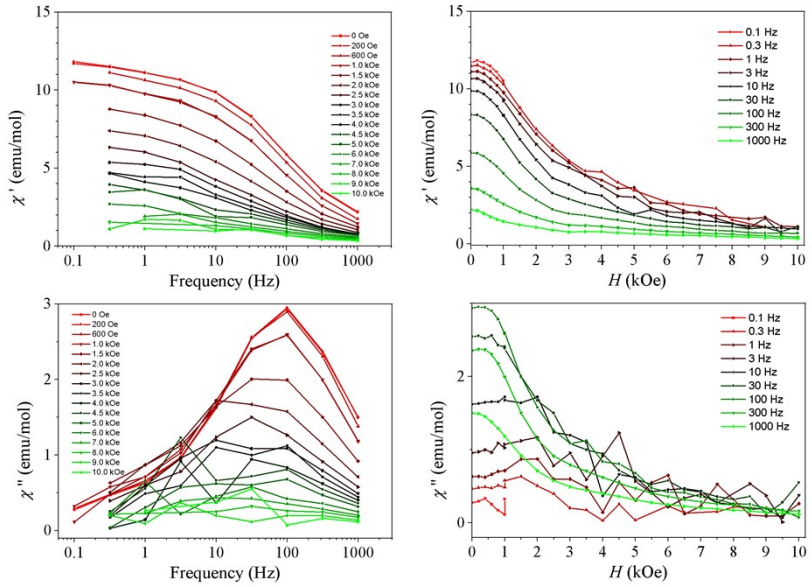

Fig. S12. Field dependence AC magnetic data for complex **3** at temperature T = 2 K.

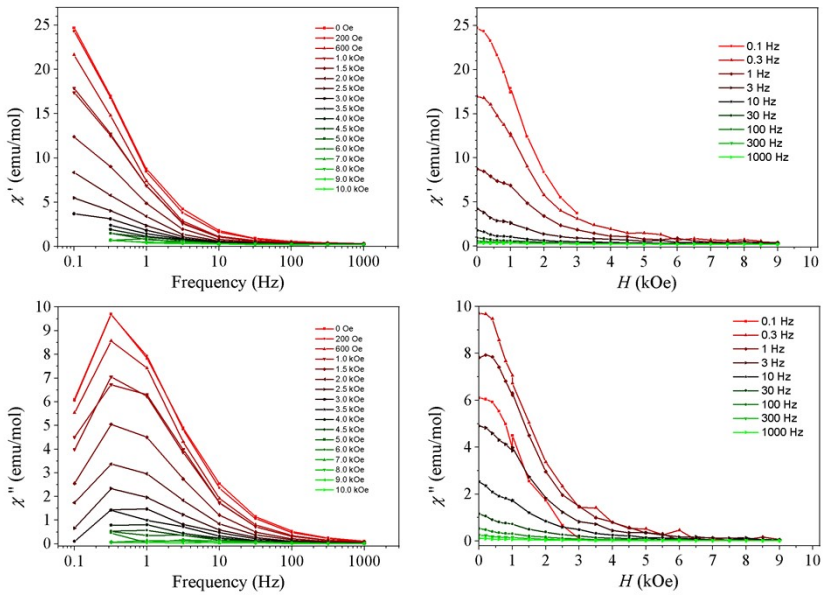

Fig. S13. Field dependence AC magnetic data for complex **4** at temperature T = 2 K.

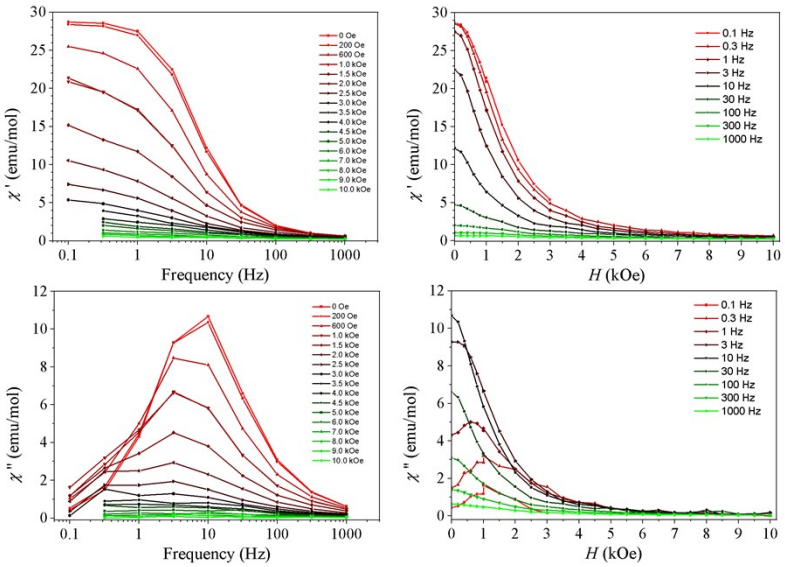

Fig. S14. Field dependence AC magnetic data for complex **5** at temperature T = 2 K.

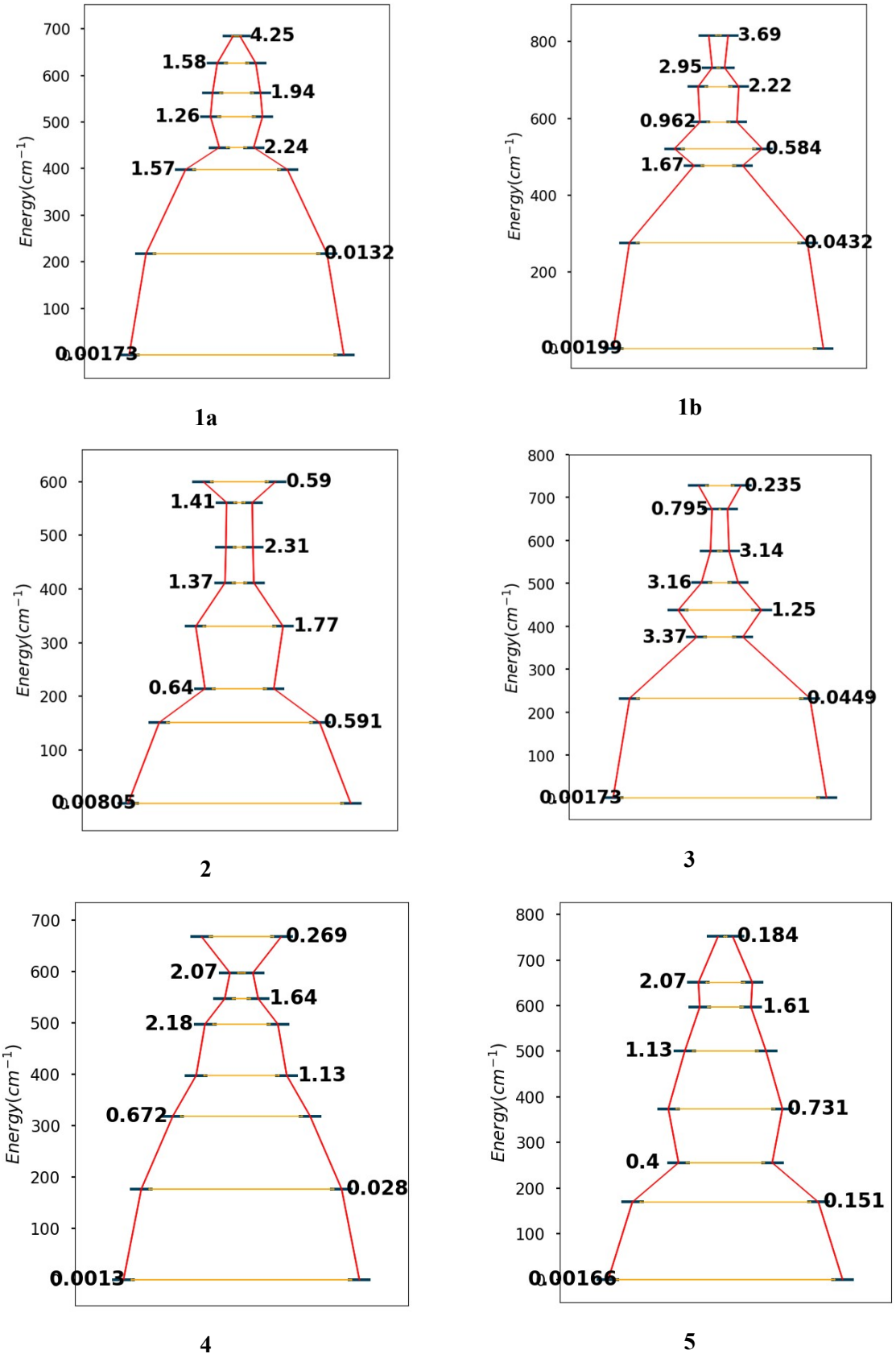

Figure S15. CASSCF calculated double-well potential for the Dy^{III} centers of **1-5**. Magnetic transition moments between states belonging to the same Kramers doublet are presented.

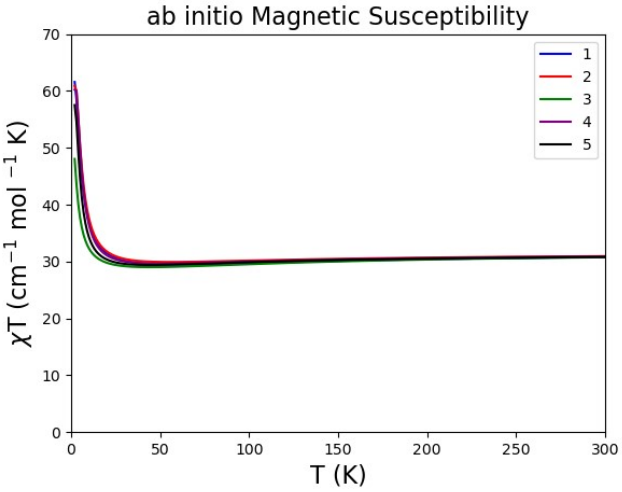

Figure S16. Magnetic susceptibility of **1-5**, calculated based on the Lines model for the exchange interaction and single-ion anisotropy based on the CASSCF results.